Title
Investigation of human brain hemodynamics by simultaneous near-infrared spectroscopy and functional magnetic resonance imaging

Journal
Medical Physics, 28(4)

ISSN
0094-2405

Authors
Toronov, Vladislav
Webb, Andrew
Choi, Jee Hyun
et al.

Publication Date
2001-04-01

DOI
10.1118/1.1354627

Medical Physics
The International Journal of Medical Physics Research and Practice

Investigation of human brain hemodynamics by simultaneous near-infrared spectroscopy and functional magnetic resonance imaging

Vladislav Toronov, Andrew Webb, Jee Hyun Choi, Martin Wolf, Antoios Michalos, Enrico Gratton, and Dennis Hueber

Citation: Medical Physics **28**, 521 (2001); doi: 10.1118/1.1354627
View online: http://dx.doi.org/10.1118/1.1354627
View Table of Contents: http://scitation.aip.org/content/aapm/journal/medphys/28/4?ver=pdfcov
Published by the American Association of Physicists in Medicine

Investigation of human brain hemodynamics by simultaneous near-infrared spectroscopy and functional magnetic resonance imaging

Vladislav Toronov,[a] Andrew Webb, and Jee Hyun Choi
Beckman Institute for Advanced Science and Technology, University of Illinois at Urbana-Champaign, 405 North Mathews, Urbana, Illinois 61801

Martin Wolf, Antoios Michalos, and Enrico Gratton
Laboratory for Fluorescence Dynamics, Department of Physics, University of Illinois at Urbana-Champaign, 1110 West Green Street, Urbana, Illinois 61801

Dennis Hueber
ISS, Incorporated, 2604 North Mattis Avenue, Champaign, Illinois 61821

(Received 2 August 2000; accepted for publication 8 January 2001)

The aim of this study was to compare functional cerebral hemodynamic signals obtained simultaneously by near infrared spectroscopy (NIRS) and by functional magnetic resonance imaging (fMRI). The contribution of superficial layers (skin and skull) to the NIRS signal was also assessed. Both methods were used to generate functional maps of the motor cortex area during a periodic sequence of stimulation by finger motion and rest. In all subjects we found a good collocation of the brain activity centers revealed by both methods. We also found a high temporal correlation between the BOLD signal (fMRI) and the deoxy-hemoglobin concentration (NIRS) in the subjects who exhibited low fluctuations in superficial head tissues. © *2001 American Association of Physicists in Medicine.* [DOI: 10.1118/1.1354627]

Key words: brain imaging, fMRI, near infrared

I. INTRODUCTION

In recent years near-infrared spectroscopy (NIRS) has been proposed as a method to study brain hemodynamics, which is simple and inexpensive compared to such ''heavy-duty'' methods as functional magnetic resonance imaging (fMRI) and positron emission tomography (PET). Many studies about applying NIRS to monitor functional cerebral hemodynamics were reviewed in Ref. 1. However, the precise location of tissues contributing to the optical signals is still uncertain. This issue can be clarified using coregistration of brain hemodynamics by NIRS and fMRI, because the blood oxygenation level dependent (BOLD) signal employed in fMRI is proportional to the changes in deoxy-hemoglobin concentration. In several studies functional brain activity was monitored separately by NIRS and fMRI in the same subjects.[2,3] However, due to strong biological fluctuations in both NIRS and fMRI signals, such a separate monitoring makes it difficult to compare the signals directly. We only know one paper describing simultaneous NIRS and MRI recordings of cerebral blood oxygenation during functional stimulation.[4] Using a continuous-wave NIRS instrument with one source-detector pair, the authors demonstrated spatial congruence between the area on the surface of the head where NIRS deoxy-hemoglobin signal was maximal and the focus of the MRI signal in the motor cortex related to the finger-movement task. However, since Kleinschmidt *et al.* employed only one slice in their fMRI setup, the contribution of extracranial artifacts to the hemodynamic changes measured by NIRS remained unclear. Furthermore, their instrument with only one source-detector pair did not allow determining differences between hemodynamic changes in the activated area and outside of it. The aim of our paper is to address these questions.

In our study we use motor stimulations to evoke functional cerebral hemodynamic changes, a multichannel frequency-domain NIRS instrument, and a set of five fMRI slices at different depths of the head from the skin to the gray matter.

II. INSTRUMENTATION AND EXPERIMENTAL PROTOCOL

For NIRS measurements we use a two-wavelength (758 and 830 nm) frequency-domain (110 MHz modulation frequency) Oximeter (ISS, Champaign, IL), which has 16 laser diodes (eight per each wavelength) and two photomultiplier tube detectors. At a wavelength of 758 nm light absorption by the deoxy-hemoglobin (HHb) substantially exceeds absorption by the oxy-hemoglobin (O_2Hb), while at 830 nm the O_2Hb absorption prevails over the HHb absorption. The laser diodes operate in a sequential multiplexing mode with 10 ms ''on'' time per each diode. Light emitted by these laser diodes is guided to the tissue through 10-meter long multimode silica optical fibers. Two 10-m long glass fiber bundles collect the scattered light and bring it to the detectors. The paired (758 and 830 nm wavelength) source fibers are attached to the probe at eight positions. Together with two detectors, they provide 10 bi-wavelength source-detector channels with a source-detector distance of 3 cm. The probe covers an area 9×6 cm^2. The geometric layout of the optical probe and its position on the head are shown in Fig. 1. The numbers 1 through 8 correspond to the light sources and the

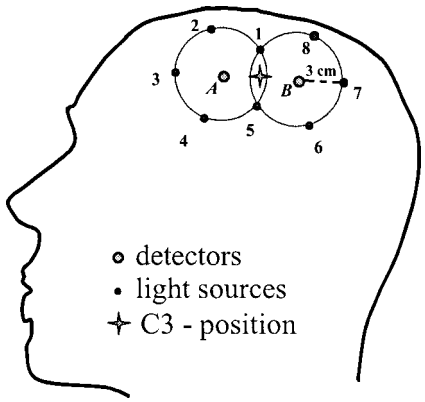

FIG. 1. Geometric layout of the optical probe and its position on the head.

letters *A* and *B* to the detectors. Using these notations, in this paper we denote the source-detector light channels as *A*1, *A*2 and so on through *B*8. The probe is centered at the measured C3 position according to the International 10–20 System.[5] Three multimodality radiological markers (IZI Medical Products Corp, Baltimore, MD) are embedded into the optical probe to facilitate correct orientation of the MRI slices with respect to the probe and to enable recovery of the probe orientation for data analysis.

Magnetic resonance imaging was performed using a 1.5 Tesla whole body MR scanner (Signa, General Electric Medical Systems, Milwaukee, WI) equipped with echospeed gradients and a standard circularly polarized birdcage headcoil. Sagittal T1-weighted localizer scans were used to determine the correct plane for the functional scans. Gradient-echo echo-planar images were acquired using a data matrix of 64×64 complex points, TR=640 ms, TE=40 ms, FOV =240 mm, slice thickness=7 mm, no interslice gap, receiver bandwidth 62.5 kHz, and tip angle 90 degrees. Figure 2 shows the arrangement of a typical set of five slices denoted as α, β, γ, δ, and ϵ. The slices are parallel to the plane of three radiological markers on the optical probe. The middle slice γ was set between the skull and the brain surface at the C3 position. This slice was mostly filled with the cerebrospinal fluid (CSF), dura mater, arachnoidal tissue, and pia mater, but also could touch the cortical tissue depending on

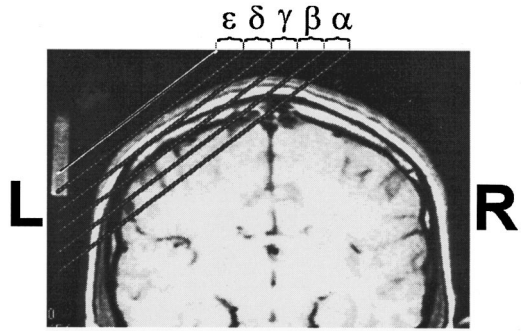

FIG. 2. Coronal anatomical image of the human head with a typical set of fMRI slices labeled as α, β, γ, δ, and ϵ. The lines show the limits of each slice. Letters ''**L**'' and ''**R**'' indicate orientation and stand for ''left'' and ''right'' correspondingly.

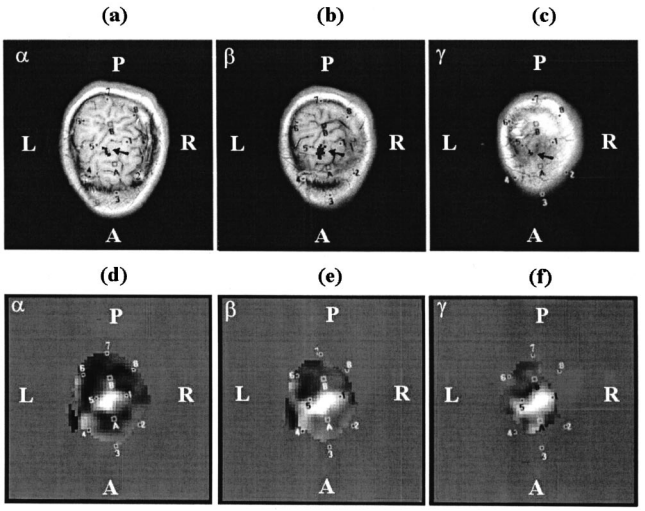

FIG. 3. (a), (b), and (c) are anatomical images corresponding to the three deepest slices α, β, and γ shown in Fig. 2. The numbers 1 through 8 number the locations of sources shown by dark dots and the letters *A* and *B* label the detectors depicted as empty squares. (d), (e), and (f) are correlation coefficient maps of the functional signals for the slices α, β, and γ shown in Figs. 3(a), 3(b), and 3(c) correspondingly. Letters ''**L**,'' ''**R**,'' ''**A**,'' and ''**P**'' indicate orientation and stand for ''left,'' ''right,'' ''anterior,'' and ''posterior,'' respectively.

the subject's anatomy. Two deeper slices, α and β, mostly contained the brain tissue, while two outer slices, δ and ϵ, included the skull, the skin and the markers (see Fig. 2). Figures 3(a), 3(b), and 3(c) represent the anatomical images corresponding to the three deepest slices α, β, and γ shown in Fig. 2. The numbers 1 through 8 show the source locations and the letters *A* and *B* indicate the detectors.

The studies were performed in six healthy right-handed male volunteers, 18 to 37 years old. Informed consent was obtained from all subjects. Each exercise run consisted of a 30-s pre-exercise epoch, ten 20-s stimulation epochs separated by ten 20-s control epochs, and a 50-s after-exercise epoch. Thus, the stimulation period was 40 s, which corresponds to 0.025 Hz in the frequency domain. During stimulation epochs subjects performed light palm squeezing with the right hand with the frequency about 1.25 Hz following the rhythm presented by the sound from the vacuum pump of the MRI scanner. This rhythm was selected to maintain the same amount of finger movements (about 50) per stimulation period. The commands to begin and to stop the exercise were presented via the speaker installed in the scanner room and by a light, which was on during the exercise epoch and off during the control epoch. 750 images acquired during each run resulted in an 8-min scan time. The synchronization of the exercise sequence with the MRI and NIRS recording was provided by a computer program generating the commands for the subject and the scanner operator based on the preset command timing.

III. SIGNAL ANALYSIS

To convert optical intensity data into hemodynamic concentration changes, we used a model of light transport in

strongly scattering medium based on the modified Lambert–Beer law.[1] We assumed that the changes in the light intensity occurred mainly due to the absorption changes rather than due to the scattering ones and that the absorption variations in the tissue were caused only by changes in HHb and O_2Hb concentrations. The modified Lambert–Beer law gives the following equation to compute the change in the absorption coefficient $\Delta\mu_a^\lambda$ at a given wavelength λ from the initial intensity $I_{\lambda 0}$ and the current intensity I_λ:

$$\Delta\mu_a^\lambda = -\frac{\ln(I_\lambda/I_{\lambda 0})}{d\sigma_\lambda}, \tag{1}$$

where d is the distance between the source and the detector fibers, and σ_λ is the differential pathlength factor (DPF). We use DPF values for the adult head of 6.2 at 758 nm and 5.9 at 830 nm (Ref. 6). The DPF dependence on the wavelength reflects a weak wavelength dependence of the tissue scattering. To avoid noise from the ambient light, we use the amplitude (AC) of the intensity-modulated light as the source data for I_λ. Changes of $[O_2Hb]$ and [HHb] corresponding to the changes in the absorption coefficients $\Delta\mu_a^{\lambda 1,2}$ of the tissue at the wavelengths λ_1 and λ_2 can be obtained using the equations[7]

$$\Delta[\mathrm{HbO2}] = \frac{\Delta\mu_a^{\lambda 1}\epsilon_{\mathrm{Hb}}^{\lambda 2} - \Delta\mu_a^{\lambda 2}\epsilon_{\mathrm{Hb}}^{\lambda 1}}{\epsilon_{\mathrm{HbO2}}^{\lambda 1}\epsilon_{\mathrm{Hb}}^{\lambda 2} - \epsilon_{\mathrm{Hb}}^{\lambda 1}\epsilon_{\mathrm{HbO2}}^{\lambda 2}}, \tag{2}$$

$$\Delta[\mathrm{Hb}] = \frac{\Delta\mu_a^{\lambda 2}\epsilon_{\mathrm{HbO2}}^{\lambda 1} - \Delta\mu_a^{\lambda 1}\epsilon_{\mathrm{HbO2}}^{\lambda 2}}{\epsilon_{\mathrm{HbO2}}^{\lambda 1}\epsilon_{\mathrm{Hb}}^{\lambda 2} - \epsilon_{\mathrm{Hb}}^{\lambda 1}\epsilon_{\mathrm{HbO2}}^{\lambda 2}}. \tag{3}$$

Here $\epsilon_{\mathrm{HHb}}^{\lambda 1,2}$ and $\epsilon_{\mathrm{O2Hb}}^{\lambda 1,2}$ are the extinction coefficients[8] of HHb and O_2Hb, respectively, at wavelengths λ_1 and λ_2.

Equations (1), (2), and (3) are derived assuming homogeneity of the scattering medium, and therefore they are not expected to provide accurate quantitative intracranial hemodynamics assessment. We do not aim at quantifying the absolute hemodynamic changes in the motor cortex, but rather we aim at the analysis of temporal characteristics, changes in [HHb] relative to changes in $[O_2Hb]$, and relative changes in different regions of the cortex. For this reason we quantify [HHb] and $[O_2Hb]$ changes by arbitrary units, which correspond to μM under the hypothetical assumption of homogeneity of tissue optical properties.

The time series obtained from the optical data using Eqs. (2) and (3) were bandpass filtered to exclude fluctuations of the time scale faster than 2 s and to eliminate the changes of the time periods significantly (approximately three times) longer than the stimulation/relaxation period.

Assuming synchronization between stimulation and hemoglobin response, we separate the functional response from background fluctuations by means of a folding average (time-locked average[4]), i.e., the data corresponding to the same point on the stimulation/relaxation cycle is averaged over a number of cycles. The beginning of the time-locked period was chosen in the middle of the relaxation epoch.

The analysis of the fMRI data was performed using MEDx software (Sensor Systems, Inc). Prior to the statistical analysis, the data was subjected to the motion detection, spatial and temporal filtering, and global intensity normalization. Data with significant motion artifacts were discarded and measurements repeated. The resulting statistical images show the maps of coefficient **r** measuring correlation between voxel BOLD intensity and a reference function. As the reference function we used either the boxcar paradigm function with the ''ON'' and ''OFF'' durations equal to the stimulation and relaxation phases of the exercise, or the [HHb] signal obtained by NIRS taken with the opposite sign.

IV. RESULTS

A. BOLD signal

In all subjects the analysis of the BOLD signal revealed an area under the optical probe where the signal was highly correlated with the paradigm boxcar function. It was an area in the primary motor cortex with the center close to the central sulcus. The size of this area varied depending on the slice. Figures 3(d), 3(e), and 3(f) show the typical correlation coefficient maps of the functional signals for the slices α, β, and γ shown in Figs. 3(a), 3(b), and 3(c) correspondingly. White color of the highest intensity corresponds to the voxels with **r** greater than 0.5 (correlation z score larger than 9.0). Correlation z score is the voxel correlation coefficient divided by the standard deviation of the distribution of correlation coefficients over the whole image. It represents a significance of correlation in the given voxel relative to the voxels whose correlation is within standard deviation from the average one. Usually, the largest size of the activated area was in the middle slice γ [see Fig. 3(f)]. In the next slice deeper in the brain β, which was mostly cortical tissue, the activation area was almost as large as in the middle slice [Fig. 3(e)]. The deepest slice α [see Fig. 3(d)] typically showed a significantly smaller activation area. Using head landmarks for the C3 position, the center of the optical probe was placed very close to the central sulcus so that light channels $A1$, $A5$, $B1$, and $B5$ were above the activated area (see Fig. 3). In two subjects the probe center was displaced from the central sulcus by 1.5–2 cm toward the frontal lobe, and the major activated area appeared under the channels $B5$, $B6$, $B7$, and $B8$. In two upper slices δ and ϵ the coefficient of correlation between BOLD signal and the paradigm function was typically less than 0.1 and the corresponding z score was less than 2.0. Figure 4(a) shows a BOLD signal from the slice β [see Fig. 3(e)] with $r=0.7$, z score of 12.5.

B. NIRS signals

Figures 4(b) and 4(c) show, respectively, the [HHb] and the $[O_2Hb]$ signals from the light channel $A5$ (Fig. 3) acquired simultaneously with the BOLD signal shown in Fig. 4(a). One can see that the directions of changes in BOLD and [HHb] signals are almost perfectly opposite. In three subjects the task-related changes were superimposed with the significant hemodynamic fluctuations in the upper tissue layers corresponding to slices δ and ϵ. However, in all subjects the folding average analysis revealed the same type of $[O_2Hb]$

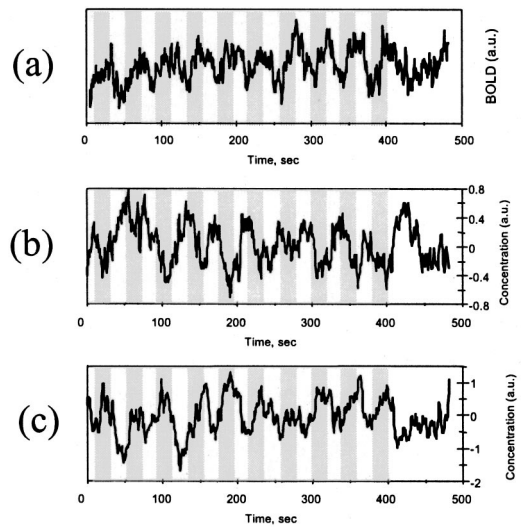

FIG. 4. (a) BOLD signal from the slice β [see Fig. 3(e)] with $r=0.7$, z score of 12.5; (b) and (c) [HHb] and [O_2Hb] signals, respectively, from the light channel $A5$ acquired simultaneously with the BOLD signal shown in (a).

and [HHb] behavior for light channels situated above the major activated area. Figure 5 shows a map of folding average [HHb] and [O_2Hb] traces acquired simultaneously with the fMRI maps presented in Fig. 3. For the light channels situated above the activated area (channels $A1$ and $A5$), the characteristic feature was a significant decrease of [HHb] during the stimulation, which was concurrent with a significant increase of the oxy-hemoglobin concentration. Typically rapid changes in [HHb] and [O_2Hb] began 2–3 s after the stimulation onset and continued during next 7–15 s. The maximal task-related change in [O_2Hb] occurred from 0.5 to 4 s before the maximal change in [HHb]. Then [HHb] fluctuated near its low level for the rest of the stimulation epoch and the beginning of the resting epoch. After achieving its maximum, [O_2Hb] either fluctuated at its high level or exhibited a slight decrease (see channels $A1$, $A5$, and $B1$ in Fig. 5). A rapid recovery toward the baseline level begins 4–6 s after the onset of the rest epoch in both [HHb] and [O_2Hb]. Such a behavior of [HHb] and [O_2Hb] in the activated area was qualitatively the same in all six subjects. Table I summarizes the ranges of the maximal task-related changes in folding average [HHb] and [O_2Hb] traces for all subjects. The values in the columns ''[HHb] change'' (''[O_2Hb] change'') show the change from the onset of the stimulation epoch to the minimum (maximum) and the corresponding average standard errors. The average standard errors are calculated in the following way. First the standard

TABLE I. Maximal magnitudes of task-related folding average [HHb] ([O_2Hb]) changes between the value at the onset of the stimulation epoch and the minimum (maximum) (a.u.=arbitrary units corresponding approximately to μM).

Subject	[HHb] change, a.u.	[O_2Hb] change, a.u.	[HHb]/[O_2Hb]
1	0.31±0.02	0.64±0.05	0.48
2	0.30±0.01	0.51±0.05	0.59
3	0.25±0.02	0.79±0.05	0.32
4	0.12±0.01	0.58±0.08	0.21
5	0.60±0.03	0.92±0.11	0.65
6	0.34±0.03	0.79±0.11	0.43

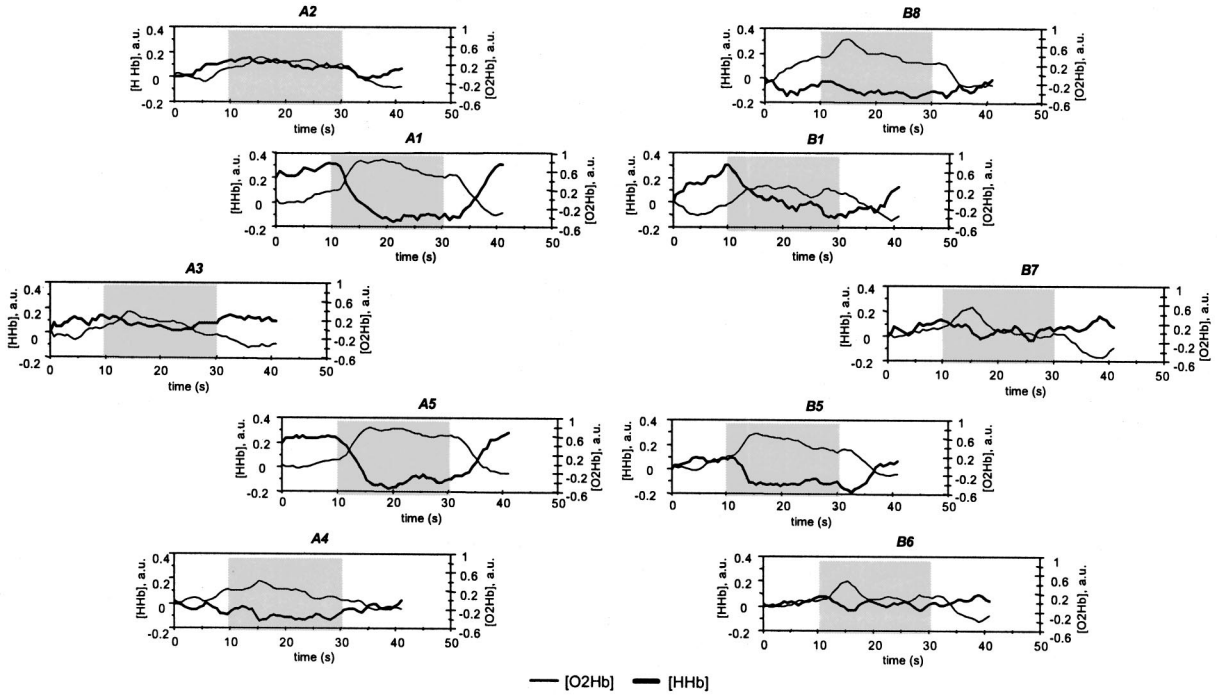

FIG. 5. A map of folding average [HHb] and [O_2Hb] traces acquired simultaneously with the fMRI maps presented in Fig. 3. The title of each panel indicates the corresponding light channel.

error for each value of [HHb] or [O_2Hb] folding-average trace is calculated by averaging over the 10 exercise periods. Then the average over the period is taken. One can see that for all subjects the task-related change exceeds the average standard error at least by a factor of 10. The values of the ratio of [HHb] and [O_2Hb] changes presented in the last column show that [HHb] changes were always smaller than the corresponding [O_2Hb] changes.

No significant decrease in the folding average [HHb] traces concurrent with the significant [O_2Hb] increase were observed during stimulations in the light channels outside the activated area. Usually [HHb] in such channels (see channels *A*2, *A*3, *A*4, *B*8, *B*7, and *B*6 in Fig. 3 and the corresponding panels in Fig. 5) fluctuated without correlation with the paradigm function. In some cases [O_2Hb] increased (see channel *B*8 in Fig. 5), but without significant [HHb] change. In two subjects both [HHb] and [O_2Hb] decreased in some channels during the stimulation indicating a decrease in blood volume in these nonactivated regions.

C. Temporal correlation between BOLD and NIRS signals

Significant changes in the folding average traces corresponding to the activated area demonstrate a correlation between the hemodynamic changes and the paradigm function. To determine the location of the tissue contributing to such a correlation we performed a correlation analysis of the BOLD signals using the inverse NIRS [HHb] signals as the reference function. ([HHb] signal was taken with the opposite sign because an increase in BOLD signal should correspond to a decrease in [HHb].) In Figs. 3(a), 3(b), and 3(c) the arrows point at the clusters of voxels where *z* score for the correlation coefficient between BOLD and [HHb] signals in channel *A*5 exceeded 10.0. One can see a good collocation of these clusters with the channel *A*5. Such a direct temporal correlation between optical and BOLD signals in cerebral and near-cerebral tissues was detected in three subjects.

D. Influence of background hemodynamic fluctuations

In other subjects the correlation coefficient between the intracranial BOLD signal and optically measured hemodynamic signals did not exceed 0.4, and the correlation images did not contain clusters of *z* scores larger than 5, although the folding average traces exhibited features similar to the ones of channels *A*1, *A*5, and *B*5 in Fig. 5 (see Fig. 6). We believe that this low temporal correlation between the intracranial BOLD and optical signals was due to strong background hemodynamic fluctuations in optical signals contributed by the superficial tissues. Such a case is illustrated in Figs. 6 and 7. Figure 6 (a) shows task-related [HHb] changes superimposed with the strong fluctuations of the period that is approximately twice as long as the task period. Because the period of fluctuations was close to the exercise period, it was difficult to effectively eliminate the corresponding fluctuations by high-pass filtering without eliminating task-related changes. Although the amplitude of the background long-

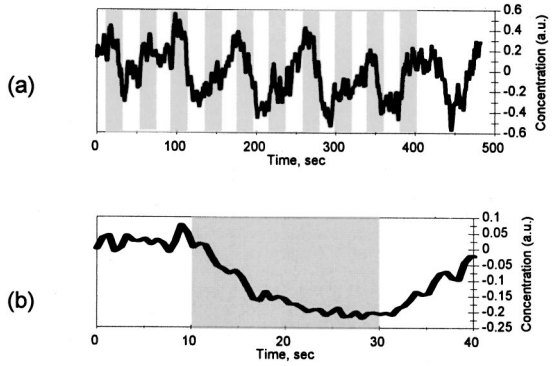

FIG. 6. (a) [HHb] trace showing strong background fluctuations; (b) folding average reveals the task-related change.

period changes is so strong that the task-related changes are almost imperceptible in the time trace in Fig. 6(a), the folding average reveals the task-related [HHb] change [Fig. 6(b)]. Figure 7(a) shows the power spectra of BOLD signals from the activated area in slice γ (thick line) and the top slice ϵ (thin line). The thick line has a high peak at the frequency corresponding to the paradigm function period (0.025 Hz), while the thin line peaks at the frequency of the background fluctuations and its harmonics. Figure 7(b) shows the spectrum of the [HHb] signal from the light channel situated above the activated area. One can see that although the [HHb] spectrum has significant power at the exercise frequency, there is a much higher peak at the frequency of the highest peak in the superficial BOLD signal [a thin line in Fig. 7(a)].

V. DISCUSSION

The decrease of [HHb] concurrent with the increase in [O_2Hb] agrees with the results of the previous simultaneous fMRI–NIRS study,[4] BOLD signal theory and with the basic knowledge of brain physiology.[9] Therefore, the collocation

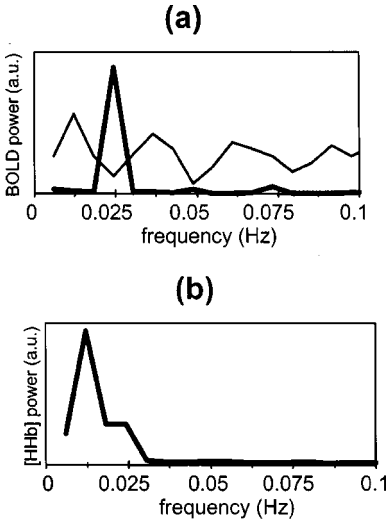

FIG. 7. (a) Power spectra of BOLD signals from the activated area in slice γ (thick line) and the top slice ϵ (thin line). (b) The spectrum of the [HHb] signal from the light channel situated above the activated area.

of the light channels exhibiting such a behavior in the folding average [HHb] and [O_2Hb] traces with the activated area revealed by fMRI in all subjects confirms that NIRS monitors the functional brain hemodynamics. Additional support for this conclusion is the temporal correlation between the intracranial BOLD signals and the respective NIRS signals. We observed such a correlation in 50% of subjects in the deep slices α, β, and γ, which included brain tissue, dura mater, pia mater, and arachnoidal tissue. The area of correlation was close to the central sulcus and collocated with the corresponding light channels. This indicates that the task-related hemodynamic changes measured by NIRS are not due to artifacts, but have intracranial origin.

Although our results on the task-related hemodynamic changes are in qualitative agreement with the ones of Kleinschmidt *et al.*,[4] there is a quantitative discrepancy in the relative magnitudes of [HHb] and [O_2Hb] changes. Kleinschmidt *et al.*[4] reported that in their measurements the [HHb] changes were larger than the [O_2Hb] ones, we always observed greater changes in [O_2Hb]. We believe that the reason for this discrepancy is a different set of wavelengths of light sources in our instrument. Kleinschmidt *et al.*[4] used a four-wavelength instrument (NIRO-500) with 775, 825, 850, and 904 nm light sources. All these wavelengths are longer than the local maximum in the [HHb] extinction coefficient at 758 nm, while in our instrument one of two wavelengths was 758 nm. This allows us to perform more accurate measurement of [HHb] changes. Another source of errors in measurements using NIRO-500 could be a high contribution of water absorption to the signal at 904 nm.

A comparison of simultaneously acquired BOLD and NIRS signals shows that in some subjects the hemodynamic fluctuations in superficial tissues at frequencies close to the exercise frequency make the detection of functional brain signals difficult and may introduce additional errors in measurements. It is a known problem in the NIRS method that the changes in superficial layers contribute much more to the overall signal change than the deep layers.[10] According to Firbank *et al.*,[10] a 1 μM change in blood concentration in the brain will give rise only to approximately 0.0005 OD change in attenuation at 3-cm source-detector distance [Fig. 9(a) in Ref. 10, no wavelength specified]. In our measurements the order of magnitude of task-related attenuation changes at both 830 nm and 758 nm was about 0.005 OD. This implies that if the estimation by Firbank *et al.*[10] is correct, the actual hemoglobin concentration change should be significantly larger than values predicted by the homogeneous model (Table I). We present changes in [HHb] and [O_2Hb] as the ones measured in ''arbitrary units'' because we believe that the layered nonhomogeneous structure of the head tissues should significantly affect the actual scale of changes calculated using the assumption of homogeneity. To achieve the quantitative accuracy in NIRS of brain hemodynamic changes one should perform the three-dimensional reconstruction of the optical properties of different tissue layers. This should also help to solve the problem of the contamination of the brain signals by superficial fluctuations. However, the three-dimensional reconstruction can only be achieved using multiple pairs of light sources and detectors separated by a variety of different distances. It cannot be applied to our data, which was acquired using the arrangement of equidistant source-detector pairs.

Another source of errors in quantitative hemodynamic measurements could be the assumption of the constancy of the scattering properties. This problem can be solved using the frequency-domain NIRS, which allows assessment of both absorption and scattering changes.

VI. CONCLUSION

Analyzing near-infrared and BOLD signals acquired simultaneously under the motor stimulation conditions, we found a good collocation between the light channels with significant task-related folding average hemodynamic changes and the functionally activated area in the motor cortex in six human subjects. A direct temporal correlation between NIRS and the intracranial BOLD signals was demonstrated in 50% of subjects. These results show the intracranial origin of the NIRS signals obtained under the periodical stimulation conditions. The lack of temporal correlation between the optical and fMRI signals in three subjects was due to the contamination of the optical signal by hemodynamic fluctuations in the superficial tissue layers. The problem of the signal contamination by superficial fluctuations and the spatial nonhomogeneity of the head tissues urge applying methods of three-dimensional reconstruction of the tissue optical properties.

ACKNOWLEDGMENTS

This work was supported by National Institutes of Health (NIH) CA57032 and RR10966.

[a]Author to whom correspondence should be addressed: Vladislav Toronov, Beckman Institute for Advanced Science and Technology, University of Illinois at Urbana-Champaign, 405 N. Mathews, Urbana, IL 61801. Electronic mail: toronov@uiuc.edu

[1] A. Villringer and B. Chance, ''Noninvasive optical spectroscopy and imaging of human brain function,'' Trends Neurosci. **20**, 435–442 (1997).

[2] G. Gratton, A. Sarno, E. Maclin, P. M. Corballis, and M. Fabiani, ''Toward non-invasive 3-D imaging of the time course of cortical activity: Investigation of the Depth of the event-related optical signal,'' Neuroimage **11**, 491–504 (2000).

[3] C. Hirth, K. Villringer, A. Thiel, J. Bernarding, W. Muhlnickl, H. Obrig, U. Dirnagl, and A. Villringer, ''Towards brain mapping combining near-infrared spectroscopy and high resolution 3D MRI,'' Adv. Exp. Med. Biol. **413**, 139–147 (1997).

[4] A. Kleinschmidt, H. Obrig, M. Requardt, K. D. Merboldt, U. Dirnagl, A. Villringer, and J. Frahm, ''Simultaneous recording of cerebral blood oxygenation changes during human brain activation by magnetic resonance imaging and near-infrared spectroscopy,'' J. Cereb. Blood Flow Metab. **16**, 817–826 (1996).

[5] H. H. Jasper, ''Report of the committee on methods of clinical examination in electroencephalography,'' Electroencephalogr. Clin. Neurophysiol. **10**, 370–375 (1957).

[6] A. Duncan, J. H. Meek, M. Clemence, C. E. Elwell, L. Tyszczuk, M. Cope, and D. T. Delpy, ''Optical pathlength measurements on adult head, calf and forearm and the head of the newborn infant using phase resolved optical spectroscopy,'' Phys. Med. Biol. **40**, 295–304 (1995).

[7] S. Fantini, M. A. Franceschini, J. S. Maier, S. A. Walker, B. Barbieri, and E. Gratton, ''Frequency-domain multichannel optical detector for noninvasive tissue spectroscopy and oximetry,'' Opt. Eng. **34**, 32–42 (1995).

[8] S. Wray, M. Cope, D. T. Delpy, J. S. Wyatt, and E. O. Reynolds, ''Characterization of the near infrared absorption spectra of cytochrome aa3 and haemoglobin for the non-invasive monitoring of cerebral oxygenation,'' Biochim. Biophys. Acta **933**, 184–192 (1988).
[9] V. S. Mattay and D. R. Weinberger, ''Organization of the human motor system as studied by functional magnetic resonance imaging,'' Eur. J. Radiol. **30**, 105–114 (1999).
[10] M. Firbank, E. Okada, and D. Delpy, ''A theoretical study of the signal contribution of regions of the adult head to near-infrared spectroscopy studies of visual evoked responses,'' Neuroimage **8**, 69–78 (1998).